

To Asymmetry and Beyond: Structured Pruning of Sequence to Sequence Models for Improved Inference Efficiency *

Daniel Campos^{1,2} and ChengXiang Zhai¹

¹Department of Computer Science, the University of Illinois Urbana-Champaign
²Neeva Inc.

Abstract

Sequence-to-sequence language models can be used to produce abstractive summaries which are coherent, relevant, and concise. Still, model sizes can make deployment in latency-sensitive or web-scale implementations difficult. This paper studies the relationship between model size, structured pruning, inference efficiency, and summarization accuracy on widely used summarization datasets. We show that model accuracy is tied to the encoder size while inference efficiency is connected to the decoder. Using asymmetric pruning can lead to nearly 3x improvement in inference latency with 1 point loss in Rouge-2. Moreover, we find both the average degradation and the role of asymmetry to be consistent across model sizes and variations in datasets. We release our code¹, training regimes, and associated model² for broad usage to encourage usage and experimentation.

1 Introduction

The application of sequence-to-sequence language models has become an important tool for natural language processing tasks such as machine translation (Sutskever et al., 2014), audio transcription (Radford et al., 2022), and abstractive summarization (Raffel et al., 2020). Sequence-to-sequence models effectively turn each of these aforementioned tasks into two-step problems: extraction and generation, and heavily condition the generation on the input.

Besides ensuring on-topic responses sequence to sequence models have the added benefit of being able to map inputs to targets with varying lengths

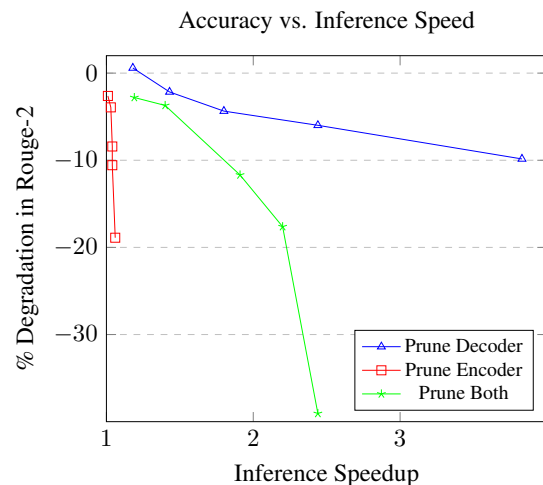


Figure 1: Impact of Asymmetrical Pruning on inference speedups and ROUGE-2 degradation on Query Independent Web Summarization. Inference Time is the mean inference time for a batch size of 1 on an A10 GPU over seven iterations.

and modalities in ways encoder or decoder-only systems cannot.

When used for abstractive summarization, sequence-to-sequence modeling has two steps, extraction using the encoder and generation using the decoder, which usually involves repeated execution until an end-of-sequence token is emitted. Since the encoder runs once on the input (Sutskever et al., 2014) its cost of execution is proportional to the batch size. The cost of decoder execution can be highly variable based on the generation length (Tay et al., 2021). Despite the broad study of sequence-to-sequence models (Raffel et al., 2020) and how they compress (Li et al., 2022), the role of model symmetry as applied to inference efficiency and model accuracy

* Corresponding author: dcampos3@illinois.edu

¹<https://github.com/spacemanidol/Efficient-Web-Scale-Abstractive-Summarization>

²<https://huggingface.co/spacemanidol>

is lacking.

Recent advances in scaling language models have led to a wide study on *scaling laws* as applied to language model performance (Kaplan et al., 2020), training data size (Hoffmann et al., 2022), machine translation (Henighan et al., 2020), and even reinforcement learning (Neumann and Gros, 2022).

We build on this work and study the impact of scaling on abstractive summarization and what role model asymmetry has in it. This asymmetry can manifest in various ways, such as the number of layers and hidden units in the encoder and decoder and the type of attention mechanisms used.

In this paper, we explore the role of asymmetry in the number of layers in encoder-decoder language modeling for summarization and its impact on the performance of these models. As shown in Figure 1, the symmetry of pruning drives the impact on accuracy and inference speedups for sequence-to-sequence models.

The following research questions drive our work:

- What scaling laws can be observed in abstractive summarization?
- What impact does encoder-decoder asymmetry have on abstractive summarization accuracy?
- What impact does encoder-decoder asymmetry have on abstractive summarization inference efficiency?
- What is asymmetries impact on accuracy and inference efficiency does scale have in encoder-decoder models for abstractive summarization?

It is in answering these questions that we deliver the following contributions:

- We present the first robust study on scaling laws applied to the compression of sequence-to-sequence modeling.
- We demonstrate that the asymmetric inference cost of sequence-to-sequence models leads to asymmetric pruning for optimal inference efficient compression.

- We empirically demonstrate on a wide variety of benchmarks how Asymmetric Compression can lead to a 2.7x inference speedup with no loss in accuracy on the XSUM dataset.

2 Related Work

Transformer Based Language Models such as BERT (Devlin et al., 2019) and T5 (Raffel et al., 2020) provide contextual language representations built on the Transformer architecture (Vaswani et al., 2017) which can be specialized and adapted for specific tasks and domains (Lee et al., 2020). Using these models, it becomes relatively easy to excel at a broad range of natural language processing tasks such as question answering, text classification, and sentiment analysis.

Scaling Laws has become an increasingly important area of study as models' size and training data grows. Performance of the transformer-based language model improves with the relation to model size (Radford, 2018) and that larger models outperform smaller models (Brown et al., 2020) on most NLP tasks. Increasing the training corpus size can lead to large improvements in performance, and model sizes can have a *optimal* training data size (Hoffmann et al., 2022). Li et al. (2020) (Li et al., 2020) explore the relationship between model size and training efficiency finding larger models train faster and are more robust to pruning and quantization (Na et al., 2022).

Asymmetrical in sequence-to-sequence models broadly refers to non-uniformity between encoder and decoder model shape or attributes. Training and inference procedures should match as closely as possible (Ranzato et al., 2015) (Mihaylova and Martins, 2019) as improvements in training loss during optimization result in improvements in model performance during Inference. While this may lead to the best model performance, it ignores the variable inference cost of sequence-to-sequence models.

During Inference, latency is dominated by the asymmetric execution of the language model. The auto-encoding encoder executes once over the entire input sequence, while the auto-regressive decoder executes iteratively until an end-of-sequence token is produced.

Kasai et al. demonstrated how the sequence-to-sequence language model performance for ma-

Table 1: Information about the architecture and attributes of the FLAN-T5 models

Model	Size(MBs)	Parameters	Encoder Layers	Parameters Encoder	Decoder Layers	Parameters decoder	Ratio End:Dec	Hidden Size
Flan-t5-small ³	146	60511616	8	35332800	8	41628352	0.849	512
Flan-t5-base ⁴	472	222903552	12	109628544	12	137949312	0.795	768
Flan-t5-large ⁵	1500	750251008	24	341231104	24	441918976	0.772	1024

chine translation is dominated by the encoder depth (Kasai et al., 2020). Tay et al. 2021 extend this work by finding a *DeepNarrow* which shows that for broad language modeling, it is possible to have 50% fewer parameters and a 40% faster inference with no loss in accuracy (Tay et al., 2021).

Efficient Inference for language modeling is a growing area of study that broadly focuses on reducing the inference cost without losses in accuracy.

Unstructured Pruning has been broadly studied (Han et al., 2015) (Sanh et al., 2020) (Kurtić et al., 2022) (Zafir et al., 2021) (Campos et al., 2022) but realizing speedups can be difficult.

Structured Pruning removes fundamental structural components in a language model such as individual attention heads (Voita et al., 2019) or entire model layers such as transformer encoders (Sanh et al., 2019). Rosenfeld et al. 2020 demonstrate that unstructured pruning impacts follow scaling laws (Rosenfeld et al., 2020) where larger models can be pruned with greater ease.

Compressing Sequence-to-sequence is a growing area of study where approaches from regular, efficient Inference has shown some transfer ability. Shleifer et al. show that it is possible to gain 1.93x speedup on a BART summarization model by applying structural pruning (Shleifer and Rush, 2020) but find compression approaches differ in their success depending on the dataset. Leveraging semi-structured pruning, Lagunas et al. can gain a 1.19 speedup (Lagunas et al., 2021) for minor losses in accuracy. While they find that the encoder is easier to prune than the decoder, they do not use this evidence of asymmetry to speed up performance further.

Li et al. investigate how to enable quantization, finding that without specialized distillation during quantization, performance collapses (Li et al., 2022). Leveraging that generation occurs iteratively, and some tokens are easier to generate than other CALM (Schuster et al., 2022) apply early exiting to improve inference speed by 1.4x. While

existing work has found interest in asymmetry, it has not been studied directly, nor has relationships in model scale been explored.

While there are other approaches such as knowledge distillation (Hinton et al., 2015) (Sanh et al., 2019) (Jiao et al., 2020), quantization (Zafir et al., 2019), early exiting (Xin et al., 2020) and token pruning (Kim et al., 2021) these are not the focus on our work as understanding the impact of many variables together limits the depth of our exploration. We leave further study of the interplay between summarization and quantization, unstructured pruning, structured pruning, and knowledge distillation for future work.

3 Scale and Abstractive Summarization

3.1 Background

Sequence-to-sequence language models such as BART (Lewis et al., 2021), T5 (Raffel et al., 2020), and PEGASUS (Zhang et al., 2020) combine transformer encoders and decoders to produce models which can adapt to novel tasks and reach top performance on tasks ranging from information retrieval (Nogueira et al., 2020) to summarization (Raffel et al., 2020).

We focus on the instruction-tuned FLAN-T5 models (Wei et al., 2021) as their performance is competitive and they feature wide variations in model size ranging from 60 million to 11 billion parameters and given the cost of training the larger variants, focus on the small, base, and large variants. Details on model size and architecture can be found in table 1.

Abstractive summarization is a method of sequence compression where a source document D is transformed into a target document d_{sum} , which is shorter but faithful to the input.

Datasets of use are a combination of public and academic benchmarks and a proprietary web search dataset. The CNN/DailyMail (CNNDM) (See et al., 2017) and XSUM (Narayan et al., 2018) datasets are based on the summarization of English new language models. The Query Independent

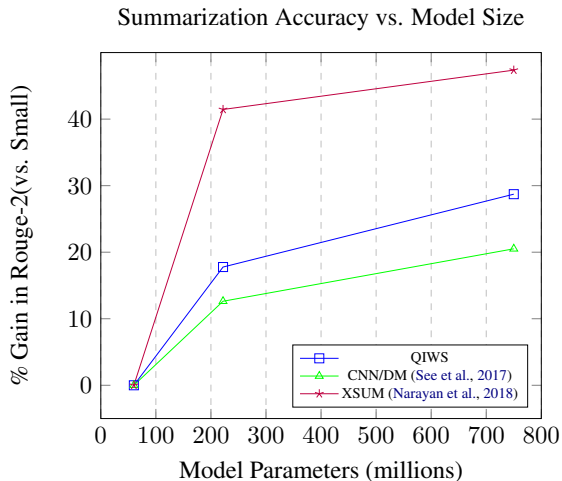


Figure 2: Model Size vs. Gain to summarization accuracy as measured by the relative Gain in rouge-2 vs. the small model.

Web Summary (QIWS) is a proprietary corpus of abstractive summaries of web pages that are used to create informative contextual snippets for search engine users. It is important to note the differences in compression factor in each dataset as each impact how decoder-driven inference latency is. Further information on the makeup of each dataset can be found in table 11.

Metrics For each dataset, we evaluate model performance by measuring the ROUGE-1 (R-1), ROUGE-2 (R-2), ROUGE-L (R-L), RougeSum-L (RSL) ⁶ (Lin, 2004), and Generation Length (GenL) on the test portion of the dataset. To aid the reproducibility and extension of our work, we experiment using HuggingFace’s Transformers ⁷, release our training and pruning scripts ⁸ and model variants for datasets that are publicly available datasets ⁹.

3.2 Scaling Laws for Abstract Summarization

To study the role of scale in abstractive summarization, we train small, base, and large models of the three datasets mentioned above. We do not study

⁶Rouge-L is sentence level vs. RougeSum-L is summary level

⁷<https://github.com/huggingface/transformers>

⁸<https://github.com/spacemanidol/Efficient-Web-Scale-Abstractive-Summarization>

⁹<https://huggingface.co/spacemanidol>

the XL (3B) and XXL (11B) as they are expensive and slow to train.

For all of our experiments, we train on various hardware but fix the batch size to 64 using gradient accumulation and leverage the hyperparameters in 12. While further hyperparameter optimization and instruction tuning would likely lead to further gains in accuracy, our work is not focused on absolute Gains but on the relative relation of scale.

As shown in 2, 13, 14, and 15, there is a substantial role between scale and performance, but there is a substantial variation across datasets.

Datasets with short candidate summaries, such as XSUM, see nearly three times the impact compared to the long summaries of QIWS and CNN/DM. During qualitative evaluations, the role of scale can easily be observed as smaller models generate more short keyword summaries while introducing scale makes responses more natural.

3.3 Inference Benchmark

To evaluate the impact of asymmetry on inference, we run experiments on the throughput of each model. Using an A10 GPU and the models from our QIWS datasets, we evaluate performance with a max sequence length of 1024, a max summary of 256, and batch sizes 1, 8, and 16 using native inference in PyTorch. We report the mean and standard deviation of timings on seven runs.

In comparing the impact of scale on R-2 vs. the effects on latency across batch sizes in 2, 4, 3 it becomes clear that larger models are more expensive to execute significantly as batch sizes increase. This is because of potential differences in output length within a batch as the batch completes when all sequences have produced an *EOS* token. To alleviate this issue bottleneck, improved streaming methods for improved batching have been proposed (Yang et al., 2020) but can be challenging to manage.

4 To Asymmetry and Beyond

While prior work has studied how to improve inference and tangentially explored the asymmetry between the encoder and decoder, we study that explicitly and across model scales. We focus our studies on **structural pruning** as inference gains are easy to realize, and this approach is highly

Table 2: Impact of scale on inference throughput for abstractive summarization models trained on the XSUM dataset. Latency is measured in MS/batch and the impact is the impact to latency vs. the small model

Model	R-2	Gain	BS 1 Latency	Impact	BS 8 Latency	Impact	BS 16 Latency	Impact
small	17.55	0.00%	138	1	230	1	330	1
base	19.77	12.63%	199	1.44	550	2.39	931	2.82
large	21.15	20.51%	445	3.22	1480	6.43	2700	8.18

Table 3: Impact of scale on inference throughput for abstractive summarization models trained on the QIWS dataset. Latency is measured in MS/batch and the impact is the impact to latency vs. the small model

Model	R-2	Gain	BS 1 Latency	Impact	BS 8 Latency	Impact	BS 16 Latency	Impact
small	29.03	0	524	1	653	1	729	1
base	34.19	17.77%	746	1.42	1060	1.62	1310	1.80
large	37.37	28.72%	1,430	2.73	2240	3.43	3320	4.55

Table 4: Impact of scale on inference throughput for abstractive summarization models trained on the CNNDM dataset. Latency is measured in MS/batch and the impact is the impact to latency vs. the small model

Model	R-2	Gain	BS 1 Latency	Impact	BS 8 Latency	Impact	BS 16 Latency	Impact
small	11.09	0	171	1.00	252	1.00	344	1.00
base	15.69	41.50%	255	1.49	550	2.18	845	2.46
large	16.34	47.41%	525	3.07	1370	5.44	2300	6.69

Table 5: Relation between scale and asymmetry on model performance on the QIWS dataset. As shown by the results in **bold** pruning only the decoder leads to less degradation than just the encoder or both, across all scales.

		Small		Base		Large	
l_{enc}	l_{dec}	R-2	R	R-2	R	R-2	R
6	6	29.03	100.00%	34.19	100.00%	37.37	100.00%
6	5	28.90	99.55%	34.00	99.44%	37.59	100.59%
6	4	28.56	98.40%	34.50	100.91%	36.56	97.84%
6	3	27.94	96.24%	33.70	98.58%	35.74	95.64%
6	2	24.85	85.61%	31.93	93.38%	35.13	94.01%
6	1	15.41	53.08%	28.05	82.03%	33.69	90.15%
5	6	27.92	96.17%	33.57	98.18%	36.39	97.38%
4	6	27.75	95.60%	33.06	96.69%	35.90	96.07%
3	6	25.20	86.82%	32.23	94.28%	34.22	91.58%
2	6	23.67	81.55%	27.47	80.35%	33.42	89.43%
1	6	18.23	62.79%	25.57	74.78%	30.31	81.11%
5	5	26.82	92.38%	32.88	96.18%	36.32	97.20%
4	4	26.62	91.72%	32.81	95.96%	35.98	96.29%
3	3	23.12	79.64%	28.70	83.95%	33.00	88.31%
2	2	19.14	65.92%	26.53	77.60%	30.78	82.38%
1	1	6.09	20.99%	19.64	57.43%	22.77	60.94%

compatible with other methods like quantization and unstructured pruning. We do not study how asymmetry is impacted by unstructured pruning or quantization as these methods are difficult to combine optimized libraries like FasterTransformers¹⁰. Following Shleifer et al., we adopt the "Shrink and then fine" (STF) tune approach for compression. First, a model is trained until convergence on a fine-tuning summarization task. Then, entire layers are removed from the encoder, decoder, or both, and the model is further fine-tuned until it has re-

converged. We do not study the use of knowledge distillation to avoid the additional training overhead without guaranteed improvements following Shleifer et al.'s results.

Each model we study has a uniform number of encoder and decoder layers, so we prune only the encoders, decoders, and a symmetric combination of the two combinations. We used our three scales of uncompressed models (small, base, large), and we pruned the model in multiples of 1 on the encoder, the decoder, and both. After pruning, models are fine-tuned again and evaluated. This means that for each dataset, we have 16 variants for each model size leading to 48 models per dataset and 144 models overall.

Given the wide number of models and the cost of multiple seeds or model-specific optimization, we train each model once and do not optimize the parameters for each model. While this leads to a worse-than-ideal performance, our goal is not to hyper-optimize models but explore where there is high sensitivity. To save space, we use the shorthand l_{enc} and l_{dec} to refer to the number portion of transformer encoder and decoder layers (out of 6), and R refers to the percentage performance recall vs. uncompressed baseline. Detailed results have been moved to the A.3 to save space.

¹⁰<https://github.com/NVIDIA/FasterTransformer>

Table 6: Relation between scale and asymmetry on model performance on the CNNDM dataset. As shown by the results in **bold** as the model size grows the impact of pruning becomes more muted

		Small		Base		Large	
l_{enc}	l_{dec}	R-2	R	R-2	R	R-2	R
6	6	17.55	100.00%	19.77	100.00%	21.15	100.00%
6	5	17.68	100.74%	19.92	100.76%	21.30	100.69%
6	4	17.27	98.36%	19.85	100.42%	21.32	100.81%
6	3	16.40	93.43%	18.85	95.37%	21.08	99.66%
6	2	15.35	87.42%	18.68	94.51%	20.67	97.73%
6	1	11.33	64.57%	16.48	83.38%	19.49	92.12%
5	6	17.69	100.81%	19.92	100.76%	21.13	99.88%
4	6	17.35	98.84%	19.67	99.50%	20.83	98.47%
3	6	16.80	95.70%	18.85	95.37%	20.53	97.06%
2	6	15.54	88.51%	18.22	92.14%	19.74	93.33%
1	6	13.31	75.83%	17.06	86.27%	18.68	88.31%
5	5	17.07	97.23%	19.72	99.74%	21.23	100.34%
4	4	16.20	92.28%	19.17	96.99%	20.90	98.81%
3	3	14.91	84.95%	17.46	88.29%	20.13	95.16%
2	2	11.97	68.17%	15.87	80.26%	18.47	87.30%
1	1	6.05	34.45%	12.23	61.88%	15.51	73.32%

Table 7: Scale and Pruning on XSUM dataset

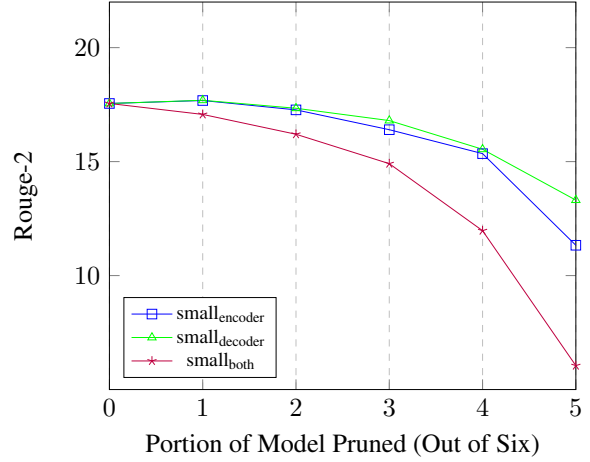
		Small		Base		Large	
l_{enc}	l_{dec}	R-2	R	R-2	R	R-2	R
6	6	11.09	100.00%	15.69	100.00%	16.34	100.00%
6	5	11.61	104.74%	15.27	97.35%	19.80	121.16%
6	4	11.43	103.12%	14.91	95.03%	19.30	118.09%
6	3	11.24	101.36%	15.40	98.17%	18.92	115.77%
6	2	10.53	94.98%	15.19	96.82%	17.96	109.93%
6	1	6.03	54.42%	13.73	87.53%	16.47	100.76%
5	6	11.18	100.82%	15.92	101.47%	19.43	118.88%
4	6	10.61	95.68%	14.10	89.91%	18.33	112.16%
3	6	10.11	91.16%	13.84	88.21%	16.90	103.39%
2	6	8.59	77.52%	12.10	77.12%	14.97	91.61%
1	6	7.70	69.43%	10.27	65.47%	12.52	76.63%
5	5	10.73	96.76%	15.72	100.22%	19.18	117.38%
4	4	10.19	91.96%	14.30	91.15%	17.56	107.43%
3	3	9.50	85.69%	12.44	79.32%	15.89	97.21%
2	2	7.31	65.91%	10.67	68.05%	12.15	74.34%
1	1	4.00	36.09%	7.74	49.35%	8.96	54.86%

4.1 Scale and Pruning

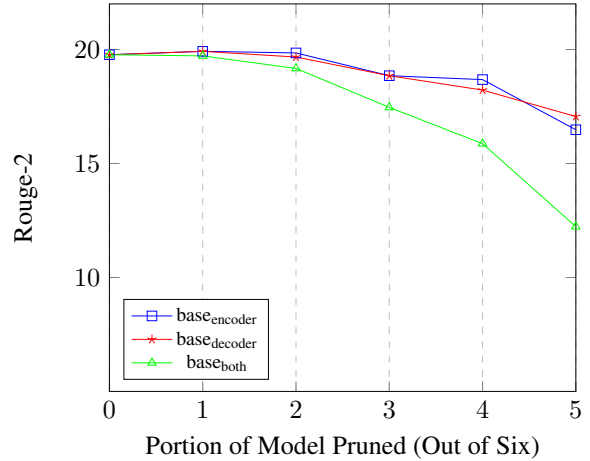
Looking at abridged results in 5, 6, and 7, there is a clear scaling law as smaller models see much larger drops in performance when compressed to the same degree. For example, on the QIWS dataset, compression to $\frac{1}{6}$ of the layers on the encoder and decoder cause an 80% drop in R-2 on a small model but only 40% on the larger model. This scale comparison is 65% to 26% on CNNDM and 64% to 45% on XSUM datasets.

Similar scaling results hold with encoder or decoder pruning, where compressing large models lead to a 5x lower loss in performance than small models. As the model’s size grows, the impact of decoder vs. encoder-only pruning becomes more muted. On the CNNDM dataset, the gap between the decoder only and encoder only pruned to $\frac{1}{6}$ is 10% with the FLAN-T5 small but only 4% with the large variant. When comparing asymmetric and symmetric, the gap is even further pronounced where the small gap is 30% while the large is 20%.

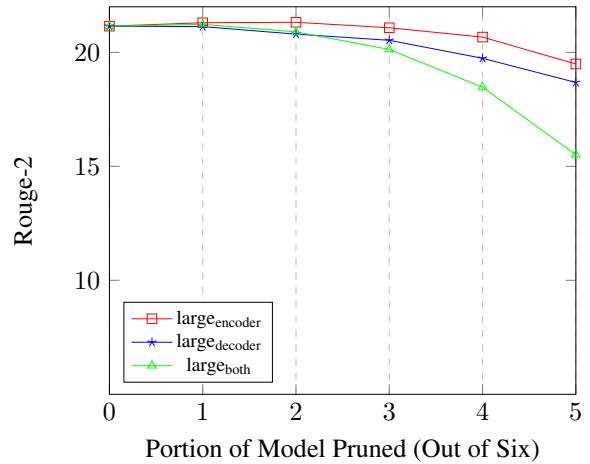
Role of scale and compression on CNNDM



Role of scale and compression on CNNDM



Role of scale and compression on CNNDM



6 Figure 3: Relationship between model compression, model size, and summarization accuracy measured by rouge-2 vs. Number Layers. $small_{encoder}$ refers to a FLAN-T5 small which has only pruned the encoder, $small_{decoder}$ for only the decoder, and $small_{both}$ for the encoder and decoder

As shown in Figure 3, the impact of compression becomes more muted as the model size grows. In other words, larger models are more compressible and amenable to asymmetry in this compression. The impact of asymmetry is easiest to understand as it is not surprising that complete pruning of a model leads to higher losses than partial pruning across datasets and model sizes. While this finding is not immediately surprising, evaluating the inference costs becomes important.

4.2 Inference Benchmarks

We evaluate the impact of asymmetry in a similar method to our scale experiments. Using an A10 GPU, we evaluate performance for summarization on a portion of each model’s respective evaluation datasets with a max sequence length of 1024, a max summary length of 256, and batch sizes 1, 8, and 16. We choose these batch sizes to represent streaming workloads (batch size 1), real-time results for the top results from a search query (batch size 8i), and max throughput given the A10’s memory budget (batch size 16)

QIWS				CNN/DailyMail				XSUM			
l_{enc}	l_{dec}	Impact	Speedup	Impact	Speedup	Impact	Speedup	Impact	Speedup		
6	3	-4.36%	1.80	-0.34%	1.65	15.77%	1.64				
6	2	-5.99%	2.44	-2.27%	2.03	9.93%	2.07				
6	1	-9.85%	3.83	-7.88%	2.70	0.76%	2.71				
3	6	-8.42%	1.04	-2.94%	1.14	3.39%	1.16				
2	6	-10.57%	1.04	-6.67%	1.19	-8.39%	1.21				
1	6	-18.89%	1.06	-11.69%	1.27	-23.37%	1.30				
3	3	-11.69%	1.91	-4.84%	1.94	-2.79%	2.06				
2	2	-17.62%	2.20	-12.70%	2.78	-25.66%	2.83				
1	1	-39.06%	2.44	-26.68%	4.96	-45.14%	4.84				

Table 8: Relationship between accuracy and speedup of encoder only, the decoder only, encoder and decoder pruning on FLAN-T5 Large models on CNN/DM, XSUM, and QIWS. Speedup is measured by comparing the improvements in latency for batch size one vs. the uncompressed baseline. The impact is the relative loss of Rouge-2 of compressed models vs. the uncompressed baseline.

Looking at the focused set of results for large models across datasets in table 8 on the impact of R-2 vs. inference speedup, we can see a clear relationship between asymmetry and inference efficiency. While detailed inference results can be found in the appendix A.4 on this focused set of results, we can see that pruning only the encoder leads to no more than 30% improvement in inference efficiency at a sizable loss in accuracy. Pruning the

model symmetrically leads to realizable inference improvements of up to 5x at the expense of summarization accuracy.

Alternatively, when only the decoder is pruned, it is possible to see most of the inference speedups seen during constant pruning with a substantially lower impact on accuracy. On the CNN/DM dataset, constant pruning leads to 8% better inference but losses nearly four times the performance of non-uniform compression.

Small				Base				Large			
l_{enc}	l_{dec}	Impact	Speedup	Impact	Speedup	Impact	Speedup	Impact	Speedup		
6	3	-3.76%	1.79	-1.42%	1.76	-4.36%	1.80				
6	2	-14.39%	2.69	-6.62%	2.13	-5.99%	2.44				
6	1	-46.92%	3.97	-17.97%	3.69	-9.85%	3.83				
3	6	-13.18%	1.02	-5.72%	1.04	-8.42%	1.04				
2	6	-18.45%	1.02	-19.65%	1.05	-10.57%	1.04				
1	6	-37.21%	1.03	-25.22%	1.06	-18.89%	1.06				
3	3	-20.36%	1.40	-16.05%	1.86	-11.69%	1.91				
2	2	-34.08%	1.30	-22.40%	2.48	-17.62%	2.20				
1	1	-79.01%	3.91	-42.57%	3.95	-39.06%	2.44				

Table 9: Relationship between accuracy and speedup of encoder only, decoder only, encoder and decoder pruning on FLAN-T5 models on QIWS concerning model size. Speedup is measured by comparing the improvements in latency for batch size one vs. the uncompressed baseline. The impact is the relative loss of Rouge-2 of compressed models vs. the uncompressed baseline.

l_{enc}	l_{dec}	Impact	Speedup (BS1)	Speedup (BS8)	Speedup (BS16)
6	3	-0.34%	1.65	1.18	1.15
6	2	-2.27%	2.03	1.25	1.22
6	1	-7.88%	2.70	1.36	1.29
3	6	-2.94%	1.14	1.48	1.54
2	6	-6.67%	1.19	1.68	1.89
1	6	-11.69%	1.27	2.21	2.43
3	3	-4.84%	1.94	1.96	1.97
2	2	-12.70%	2.78	2.88	2.92
1	1	-26.68%	4.96	5.54	5.64

Table 10: Relationship between accuracy and speedup of encoder only, decoder only, encoder and decoder pruning on FLAN-T5 large models on CNN with variation in inference batch size. Speedup is measured by comparing the improvements in latency vs. the uncompressed baseline at various batch sizes. The impact is the relative loss of Rouge-2 of compressed models vs. the uncompressed baseline.

5 Discussion

5.1 Scale, Inference, and Pruning

As shown in table 9, the gains found by pruning are extremely consistent independently with scaling.

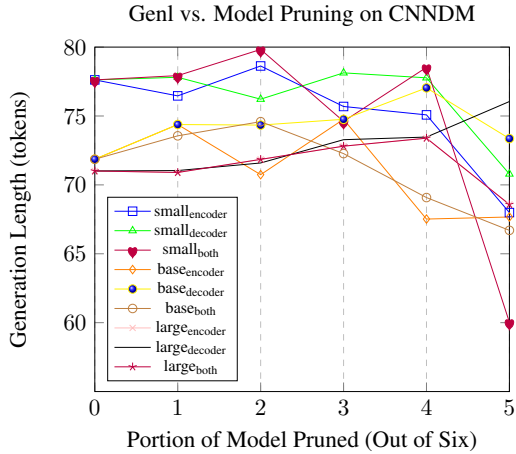


Figure 4: Role of scale and compression on generation length

Pruning only the encoder leads to a 4-6% improvement in latency, and pruning just the decoder leads to 400%, as does uniform compression. This is expected as structural pruning removes a constant portion of the network, which leads to consistent latency gains irrespective of model scale.

5.2 Scale, Pruning and Generated length

Despite expecting a significant trend in the role of scale and pruning in a generation, we do not see any noticeable trends. As shown in figures 6 and 4, there is no discernible trend of the Role of scale and pruning in generation length. There is a minor jump in generation length from FLAN-T5 small to FLAN-T5 base across all datasets but no such jump from FLAN-T5 base to FLAN-T5 large. We believe this is because the smaller models are less fluent and need more tokens to ensure accurate coverage. As models scale, this is no longer needed, and the models converge to a uniform summary length.

5.3 Asymmetry with large batches

Despite the allure of asymmetrical pruning, it is not without fault. As shown in table 10 and Figure 5, the improvements in inference efficiency are heavily influenced by the batch size. When the batch size is minimal, the difference in the type of non-uniformity has a significant impact

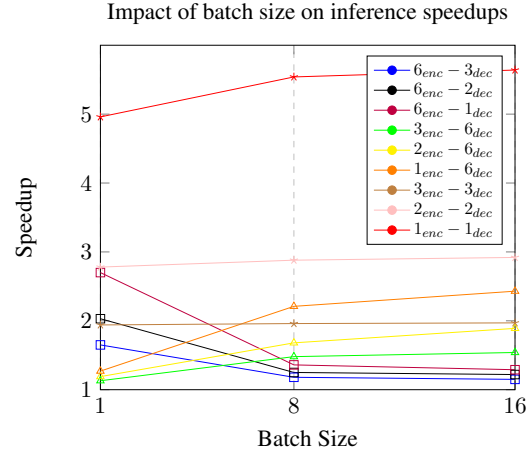


Figure 5: Relationship between inference batch size and realized inference speedup with uniform and non uniform pruning of FLAN-T5 large on CNNDM

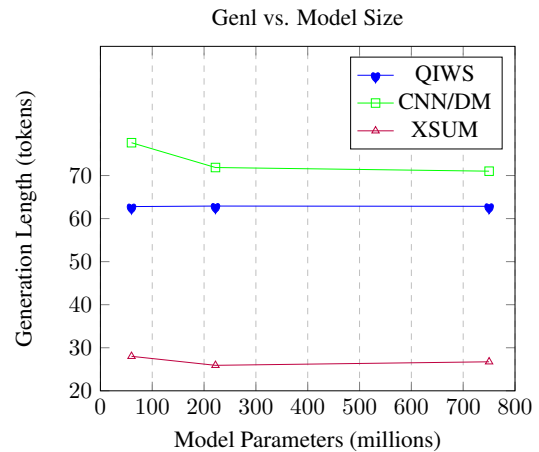


Figure 6: Role of scale on generation length

on inference efficiency. As batches scale, the speedup from encoder only or decoder only becomes much closer and becomes minor when compared to uniform methods. This indicates why further work on improving generative inference methods is highly relevant, as this problem impacts other efficiency-driven processes like CALM (Schuster et al., 2022).

6 Conclusion and Future Work

In this work, we explore the role of symmetry in the pruning of sequence-to-sequence models for abstractive summarization, finding that pruning asymmetrically can lead to inference speedups with low losses in accuracy. Our work also explores the relationship between model scale and the sensitivity to pruning, finding that larger models see lower losses when pruned. This compresses FLAN-T5 models to deliver 3x inference gains with a 1 Rouge-2 point loss.

In future work, we seek to study how pseudo labeling, early exiting, and quantization can be combined to improve further the inference efficiency of sequence-to-sequence models.

References

- Tom B. Brown, Benjamin Mann, Nick Ryder, Melanie Subbiah, Jared Kaplan, Prafulla Dhariwal, Arvind Neelakantan, Pranav Shyam, Girish Sastry, Amanda Askell, Sandhini Agarwal, Ariel Herbert-Voss, Gretchen Krueger, T. J. Henighan, Rewon Child, Aditya Ramesh, Daniel M. Ziegler, Jeff Wu, Clemens Winter, Christopher Hesse, Mark Chen, Eric Sigler, Mateusz Litwin, Scott Gray, Benjamin Chess, Jack Clark, Christopher Berner, Sam McCandlish, Alec Radford, Ilya Sutskever, and Dario Amodei. 2020. Language models are few-shot learners. *ArXiv*, abs/2005.14165.
- Daniel Fernando Campos, Alexandre Marques, Tuan Anh D. Nguyen, Mark Kurtz, and ChengXiang Zhai. 2022. Sparse*bert: Sparse models are robust. *ArXiv*, abs/2205.12452.
- J. Devlin, Ming-Wei Chang, Kenton Lee, and Kristina Toutanova. 2019. Bert: Pre-training of deep bidirectional transformers for language understanding. In *NAACL*.
- Song Han, Huizi Mao, and William J. Dally. 2015. A deep neural network compression pipeline: Pruning, quantization, huffman encoding. *ArXiv*.
- T. J. Henighan, Jared Kaplan, Mor Katz, Mark Chen, Christopher Hesse, Jacob Jackson, Heewoo Jun, Tom B. Brown, Prafulla Dhariwal, Scott Gray, Chris Hallacy, Benjamin Mann, Alec Radford, Aditya Ramesh, Nick Ryder, Daniel M. Ziegler, John Schulman, Dario Amodei, and Sam McCandlish. 2020. Scaling laws for autoregressive generative modeling. *ArXiv*, abs/2010.14701.
- Geoffrey E. Hinton, Oriol Vinyals, and J. Dean. 2015. Distilling the knowledge in a neural network. *ArXiv*, abs/1503.02531.
- Jordan Hoffmann, Sebastian Borgeaud, Arthur Mensch, Elena Buchatskaya, Trevor Cai, Eliza Rutherford, Diego de Las Casas, Lisa Anne Hendricks, Johannes Welbl, Aidan Clark, Tom Hennigan, Eric Noland, Katie Millican, George van den Driessche, Bogdan Damoc, Aurelia Guy, Simon Osindero, Karen Simonyan, Erich Elsen, Jack W. Rae, Oriol Vinyals, and L. Sifre. 2022. Training compute-optimal large language models. *ArXiv*, abs/2203.15556.
- Xiaoqi Jiao, Yichun Yin, Lifeng Shang, Xin Jiang, Xiao Chen, Linlin Li, Fang Wang, and Qun Liu. 2020. Tinybert: Distilling bert for natural language understanding. *ArXiv*, abs/1909.10351.
- Jared Kaplan, Sam McCandlish, T. J. Henighan, Tom B. Brown, Benjamin Chess, Rewon Child, Scott Gray, Alec Radford, Jeff Wu, and Dario Amodei. 2020. Scaling laws for neural language models. *ArXiv*, abs/2001.08361.
- Jungo Kasai, Nikolaos Pappas, Hao Peng, James Cross, and Noah A. Smith. 2020. Deep encoder, shallow decoder: Reevaluating non-autoregressive machine translation. In *International Conference on Learning Representations*.
- Sehoon Kim, Sheng Shen, David Thorsley, Amir Ghohami, Joseph Hassoun, and Kurt Keutzer. 2021. Learned token pruning for transformers. *Proceedings of the 28th ACM SIGKDD Conference on Knowledge Discovery and Data Mining*.
- Eldar Kurtić, Daniel Fernando Campos, Tuan Nguyen, Elias Frantar, Mark Kurtz, Ben Fineran, Michael Goin, and Dan Alistarh. 2022. The optimal bert surgeon: Scalable and accurate second-order pruning for large language models. *ArXiv*, abs/2203.07259.
- François Lagunas, Ella Charlaix, Victor Sanh, and Alexander M. Rush. 2021. Block pruning for faster transformers. *ArXiv*, abs/2109.04838.
- Jinhyuk Lee, Wonjin Yoon, Sungdong Kim, Donghyeon Kim, Sunkyu Kim, Chan Ho So, and Jaewoo Kang. 2020. Biobert: a pre-trained biomedical language representation model for biomedical text mining. *Bioinformatics*, 36:1234–1240.

- Patrick Lewis, Yuxiang Wu, Linqing Liu, Pasquale Minervini, Heinrich Küttler, Aleksandra Piktus, Pontus Stenetorp, and Sebastian Riedel. 2021. [PAQ: 65 million probably-asked questions and what you can do with them](#). *Transactions of the Association for Computational Linguistics*, 9:1098–1115.
- Zheng Li, Zijian Wang, Ming Tan, Ramesh Nallapati, Parminder Bhatia, Andrew O. Arnold, Bing Xiang, and Dan Roth. 2022. Dq-bart: Efficient sequence-to-sequence model via joint distillation and quantization. In *Annual Meeting of the Association for Computational Linguistics*.
- Zhuohan Li, Eric Wallace, Sheng Shen, Kevin Lin, K. Keutzer, D. Klein, and Joseph Gonzalez. 2020. Train large, then compress: Rethinking model size for efficient training and inference of transformers. *ArXiv*, abs/2002.11794.
- Chin-Yew Lin. 2004. [ROUGE: A package for automatic evaluation of summaries](#). In *Text Summarization Branches Out*, pages 74–81, Barcelona, Spain. Association for Computational Linguistics.
- Tsvetomila Mihaylova and André F. T. Martins. 2019. Scheduled sampling for transformers. *ArXiv*, abs/1906.07651.
- Clara Na, Sanket Vaibhav Mehta, and Emma Strubell. 2022. Train flat, then compress: Sharpness-aware minimization learns more compressible models. *ArXiv*, abs/2205.12694.
- Shashi Narayan, Shay B. Cohen, and Mirella Lapata. 2018. Don’t give me the details, just the summary! topic-aware convolutional neural networks for extreme summarization. *ArXiv*, abs/1808.08745.
- Oren Neumann and Claudius Gros. 2022. Scaling laws for a multi-agent reinforcement learning model. *ArXiv*, abs/2210.00849.
- Rodrigo Nogueira, Zhiying Jiang, Ronak Pradeep, and Jimmy J. Lin. 2020. Document ranking with a pre-trained sequence-to-sequence model. In *Findings*.
- Alec Radford. 2018. Improving language understanding by generative pre-training.
- Alec Radford, Jong Wook Kim, Tao Xu, Greg Brockman, Christine McLeavey, and Ilya Sutskever. 2022. Robust speech recognition via large-scale weak supervision. *ArXiv*, abs/2212.04356.
- Colin Raffel, Noam M. Shazeer, Adam Roberts, Katherine Lee, Sharan Narang, Michael Matena, Yanqi Zhou, Wei Li, and Peter J. Liu. 2020. Exploring the limits of transfer learning with a unified text-to-text transformer. *ArXiv*, abs/1910.10683.
- Marc’Aurelio Ranzato, Sumit Chopra, Michael Auli, and Wojciech Zaremba. 2015. Sequence level training with recurrent neural networks. *CoRR*, abs/1511.06732.
- Jonathan S. Rosenfeld, Jonathan Frankle, Michael Carbin, and Nir Shavit. 2020. On the predictability of pruning across scales. *ArXiv*, abs/2006.10621.
- Victor Sanh, Lysandre Debut, Julien Chaumond, and Thomas Wolf. 2019. Distilbert, a distilled version of bert: smaller, faster, cheaper and lighter. *arXiv preprint arXiv:1910.01108*.
- Victor Sanh, Thomas Wolf, and Alexander M. Rush. 2020. Movement pruning: Adaptive sparsity by fine-tuning. *ArXiv*, abs/2005.07683.
- Tal Schuster, Adam Fisch, Jai Gupta, Mostafa Dehghani, Dara Bahri, Vinh Quang Tran, Yi Tay, and Donald Metzler. 2022. Confident adaptive language modeling. *ArXiv*, abs/2207.07061.
- Abigail See, Peter J. Liu, and Christopher D. Manning. 2017. [Get to the point: Summarization with pointer-generator networks](#). In *Proceedings of the 55th Annual Meeting of the Association for Computational Linguistics (Volume 1: Long Papers)*, pages 1073–1083, Vancouver, Canada. Association for Computational Linguistics.
- Sam Shleifer and Alexander M. Rush. 2020. Pre-trained summarization distillation. *ArXiv*, abs/2010.13002.
- Ilya Sutskever, Oriol Vinyals, and Quoc V. Le. 2014. Sequence to sequence learning with neural networks. In *NIPS*.
- Yi Tay, Mostafa Dehghani, Jinfeng Rao, William Fedus, Samira Abnar, Hyung Won Chung, Sharan Narang, Dani Yogatama, Ashish Vaswani, and Donald Metzler. 2021. Scale efficiently: Insights from pre-training and fine-tuning transformers. *ArXiv*, abs/2109.10686.
- Ashish Vaswani, Noam M. Shazeer, Niki Parmar, Jakob Uszkoreit, Llion Jones, Aidan N. Gomez, Lukasz Kaiser, and Illia Polosukhin. 2017. Attention is all you need. *ArXiv*, abs/1706.03762.
- Elena Voita, David Talbot, F. Moiseev, Rico Sennrich, and Ivan Titov. 2019. Analyzing multi-head self-attention: Specialized heads do the heavy lifting, the rest can be pruned. In *ACL*.
- Jason Wei, Maarten Bosma, Vincent Zhao, Kelvin Guu, Adams Wei Yu, Brian Lester, Nan Du, Andrew M. Dai, and Quoc V. Le. 2021. Finetuned language models are zero-shot learners. *ArXiv*, abs/2109.01652.
- Ji Xin, Raphael Tang, Jaejun Lee, Yaoliang Yu, and Jimmy J. Lin. 2020. Deebert: Dynamic early exiting for accelerating bert inference. In *ACL*.

Kevin Yang, Violet Yao, John DeNero, and Dan Klein. 2020. A streaming approach for efficient batched beam search. In *Conference on Empirical Methods in Natural Language Processing*.

Ofir Zafrir, Guy Boudoukh, Peter Izsak, and Moshe Wasserblat. 2019. Q8bert: Quantized 8bit bert. *2019 Fifth Workshop on Energy Efficient Machine Learning and Cognitive Computing - NeurIPS Edition (EMC2-NIPS)*, pages 36–39.

Ofir Zafrir, Ariel Larey, Guy Boudoukh, Haihao Shen, and Moshe Wasserblat. 2021. Prune once for all: Sparse pre-trained language models. *ArXiv*, abs/2111.05754.

Jingqing Zhang, Yao Zhao, Mohammad Saleh, and Peter J. Liu. 2020. Pegasus: Pre-training with extracted gap-sentences for abstractive summarization. *ArXiv*, abs/1912.08777.

A Appendix

A.1 Training Details

In all of our experiments, we leverage the parameters shown in 12 on the datasets shown in 11

A.2 Scale and Abstractive summarization

The role of model scale on performance on the QIWS, CNN/DM, and XSUM datasets can be found in tables 14,13, and 15

A.3 Asymmetry in Summarization

The role of the model scale, structural pruning, and asymmetry on performance on the QIWS, CNN/DM, and XSUM datasets can be found in tables 22,23,24,16,17,18,19,20, and 21.

A.4 Inference Benchmarks

Detailed variations in latency measurements across batch size, scale, structural pruning, and asymmetry on performance on the QIWS, CNN/DM, and XSUM datasets can be found in tables 25,26, 27, 28,29, 30, 33, 31, and 32.

A.5 Responsible NLP Research - Reproducibility Checklist

A.5.1 Scientific Artifacts

Datasets. We perform our experimentation on well-established benchmarks using many broad domains and a proprietary web summarization dataset. We do not perform any modification or augmentation on public benchmarks in any dataset.

Models. The model used as a starting point for all of our experiments is the family of flan-t5 models, publicly available via HuggingFace Hub ¹³. All other models presented in this paper are openly-available in the hugging face hub.

A.5.2 Computational Experiments

Our experimentation on finetuning our compressed models uses a single 40GB A100. Finetuning time varies across datasets ranging from 1 hour for T5-small to 24 hours for T5-Large.

A.5.3 Computational Packages

All of our experimentation is done using public libraries and datasets to ensure extensibility and reproducibility. Our investigation is done using HuggingFace’s Transformers ¹⁴ and Datasets ¹⁵.

¹³<https://huggingface.co/bert-base-uncased>

¹⁴<https://github.com/huggingface/transformers>

¹⁵<https://github.com/huggingface/datasets>

Table 11: Statistics for the abstractive summarization datasets which we study. Source and Summary refer to the number of words in each, and the compression factor is the ratio between the two on the train portion of the dataset.

Dataset	Train	Validation	Test	Source	Summary	Compression
CNNDM ¹¹	287,113	13,368	11,490	691.87	51.57	14.80
XSUM ¹²	204,045	11,332	11,334	373.86	21.09	18.70
QIWS	10000	1000	1000	1410.12	73.78	19.11

HyperParameter	Value
Training Length	3,10 Epochs
Initial learning rate	1e-4
Learning rate schedule	constant
Batch size	64
Weight Decay	0.01, 0.05, 0.1

Table 12: Training Hyperparameters for summarization experiments

Model	R-1	Impact	R-2	Impact	RSL	Impact	R-L	Impact	Genl	Impact
small	50.22	0.00%	29.03	0.00%	45.87	0.00%	40.19	0.00%	62.79	0.00%
base	54.84	9.20%	34.19	17.77%	50.38	9.83%	44.68	11.18%	62.91	0.19%
large	57.81	15.11%	37.37	28.72%	53.14	15.84%	48.16	19.84%	62.85	0.10%

Table 13: Impact of Scale on summarization performance on QIWS dataset

Model	R-1	Impact	R-2	Impact	RSL	Impact	R-L	Impact	Genl	Impact
small	39.31	0.00%	17.55	0.00%	36.50	0.00%	27.97	0.00%	77.62	0.00%
base	42.14	7.20%	19.77	12.63%	39.32	7.75%	30.15	7.80%	71.86	-7.42%
large	43.99	11.90%	21.15	20.51%	41.12	12.68%	31.64	13.11%	71.01	-8.51%

Table 14: Impact of Scale on summarization performance on CNNDM dataset

Model	R-1	Impact	R-2	Impact	RSL	Impact	R-L	Impact	Genl	Impact
small	33.2675	0.00%	11.09	0.00%	26.17	0.00%	26.17	0.00%	28.01	0.00%
base	38.7782	16.56%	15.69	41.45%	31.14	19.01%	31.15	19.04%	25.92	-7.48%
large	39.7125	19.36%	16.34	47.36%	31.72	21.21%	31.72	21.23%	26.74	-4.54%

Table 15: Impact of Scale on summarization performance on XSUM dataset

Table 16: The relation between pruning asymmetry and symmetry for a FLAN-T5 small model on the CNN/DailyMail Abstractive Summarization Dataset

l_{enc}	l_{dec}	R-1	Impact	R-2	Impact	RSL	Impact	R-L	Impact	GenL	Impact
8	8	39.31	0.00%	17.55	0.00%	36.50	0.00%	27.97	0.00%	77.62	0.00%
8	6	39.33	0.04%	17.68	0.74%	36.54	0.13%	28.21	0.87%	76.46	-1.49%
8	5	38.75	-1.42%	17.27	-1.64%	36.01	-1.32%	27.91	-0.23%	78.63	1.31%
8	4	37.18	-5.42%	16.40	-6.57%	34.46	-5.58%	27.22	-2.70%	75.69	-2.48%
8	2	35.47	-9.76%	15.35	-12.58%	32.78	-10.17%	26.28	-6.06%	75.08	-3.27%
8	1	29.27	-25.55%	11.33	-35.43%	26.97	-26.09%	22.33	-20.18%	67.99	-12.40%
6	8	39.59	0.71%	17.69	0.81%	36.80	0.83%	28.08	0.39%	77.81	0.25%
5	8	39.12	-0.47%	17.35	-1.16%	36.38	-0.31%	27.73	-0.88%	76.22	-1.80%
4	8	38.57	-1.87%	16.80	-4.30%	35.79	-1.92%	27.15	-2.92%	78.13	0.67%
2	8	36.82	-6.32%	15.54	-11.49%	34.00	-6.84%	25.79	-7.78%	77.77	0.20%
1	8	33.58	-14.58%	13.31	-24.17%	30.96	-15.16%	23.72	-15.19%	70.79	-8.79%
6	6	38.59	-1.82%	17.07	-2.77%	35.80	-1.91%	27.55	-1.52%	77.93	0.41%
5	5	37.31	-5.08%	16.20	-7.72%	34.60	-5.19%	26.83	-4.07%	79.83	2.85%
4	4	35.28	-10.25%	14.91	-15.05%	32.54	-10.85%	25.74	-7.98%	74.61	-3.88%
2	2	30.79	-21.66%	11.97	-31.83%	28.03	-23.19%	22.88	-18.19%	78.53	1.18%
1	1	21.30	-45.80%	6.05	-65.55%	19.57	-46.39%	16.62	-40.56%	60.03	-22.66%

Table 17: The relation between pruning asymmetry and symmetry for a FLAN-T5 base model on the CNN/DailyMail Abstractive Summarization Dataset

l_{enc}	l_{dec}	R-1	Impact	R-2	Impact	RSL	Impact	R-L	Impact	GenL	Impact
12	12	42.14	0.00%	19.77	0.00%	39.32	0.00%	30.15	0.00%	71.86	0.00%
12	10	42.49	0.84%	19.92	0.76%	39.62	0.75%	30.27	0.40%	74.38	3.51%
12	8	42.28	0.34%	19.85	0.42%	39.48	0.41%	30.35	0.64%	70.74	-1.56%
12	6	41.30	-1.99%	18.85	-4.63%	38.44	-2.25%	29.16	-3.28%	74.76	4.04%
12	4	40.31	-4.34%	18.68	-5.49%	37.71	-4.10%	29.45	-2.33%	67.52	-6.04%
12	2	36.75	-12.80%	16.48	-16.62%	34.22	-12.97%	27.61	-8.43%	67.67	-5.82%
10	12	42.49	0.84%	19.92	0.76%	39.62	0.75%	30.27	0.40%	74.38	3.51%
8	12	42.27	0.31%	19.67	-0.50%	39.41	0.22%	29.99	-0.52%	74.34	3.45%
6	12	41.30	-1.99%	18.85	-4.63%	38.44	-2.25%	29.16	-3.28%	74.76	4.04%
4	12	40.51	-3.86%	18.22	-7.86%	37.66	-4.23%	28.42	-5.75%	77.04	7.21%
2	12	39.03	-7.38%	17.06	-13.73%	36.15	-8.08%	27.23	-9.69%	73.36	2.09%
10	10	42.19	0.13%	19.72	-0.26%	39.38	0.14%	30.12	-0.11%	73.56	2.37%
8	8	41.64	-1.18%	19.17	-3.01%	38.83	-1.26%	29.60	-1.84%	74.59	3.80%
6	6	39.33	-6.67%	17.46	-11.71%	36.67	-6.74%	28.07	-6.92%	72.27	0.57%
4	4	36.99	-12.23%	15.87	-19.74%	34.43	-12.43%	26.63	-11.68%	69.08	-3.87%
2	2	30.99	-26.45%	12.23	-38.12%	28.43	-27.71%	23.28	-22.79%	66.70	-7.18%

Table 18: The relation between pruning asymmetry and symmetry for a FLAN-T5 large model on the CNN/DailyMail Abstractive Summarization Dataset

l_{enc}	l_{dec}	R-1	Impact	R-2	Impact	RSL	Impact	R-L	Impact	GenL	Impact
24	24	43.99	0.00%	21.15	0.00%	41.12	0.00%	31.64	0.00%	71.01	0.00%
24	20	44.15	0.37%	21.30	0.69%	41.31	0.46%	31.73	0.31%	71.20	0.26%
24	16	44.10	0.27%	21.32	0.81%	41.29	0.39%	31.83	0.60%	70.19	-1.16%
24	12	43.74	-0.57%	21.08	-0.34%	40.97	-0.38%	31.60	-0.13%	69.99	-1.44%
24	8	43.35	-1.45%	20.67	-2.27%	40.58	-1.32%	31.29	-1.11%	72.88	2.63%
24	4	41.42	-5.84%	19.49	-7.88%	38.78	-5.69%	30.35	-4.06%	70.39	-0.89%
20	24	44.10	0.26%	21.13	-0.12%	41.28	0.38%	31.58	-0.17%	71.04	0.04%
16	24	43.76	-0.52%	20.83	-1.53%	40.92	-0.49%	31.22	-1.31%	71.59	0.80%
12	24	43.33	-1.50%	20.53	-2.94%	40.43	-1.68%	30.82	-2.58%	73.28	3.20%
8	24	42.46	-3.48%	19.74	-6.67%	39.64	-3.60%	29.98	-5.23%	73.47	3.46%
4	24	41.25	-6.23%	18.68	-11.69%	38.30	-6.86%	28.78	-9.04%	76.05	7.08%
20	20	44.10	0.25%	21.23	0.34%	41.25	0.32%	31.65	0.05%	70.90	-0.16%
16	16	43.69	-0.67%	20.90	-1.19%	40.86	-0.64%	31.30	-1.06%	71.85	1.18%
12	12	42.81	-2.67%	20.13	-4.84%	39.97	-2.80%	30.58	-3.33%	72.81	2.53%
8	8	40.57	-7.78%	18.47	-12.70%	37.82	-8.04%	28.96	-8.46%	73.39	3.34%
4	4	36.11	-17.91%	15.51	-26.68%	33.48	-18.59%	26.30	-16.88%	68.58	-3.43%

Table 19: The relation between pruning asymmetry and symmetry for a FLAN-T5 small model on the Query Independent Web Snippets Abstractive Summarization Dataset

l_{enc}	l_{dec}	R-1	Impact	R-2	Impact	RSL	Impact	R-L	Impact	GenL	Impact
8	8	50.22	100.00%	29.03	100.00%	45.87	100.00%	40.19	100.00%	62.79	100.00%
8	6	50.20	99.96%	28.90	99.55%	45.80	99.83%	40.45	100.65%	62.81	100.03%
8	5	49.74	99.04%	28.56	98.40%	45.55	99.30%	40.27	100.20%	62.68	99.83%
8	4	48.59	96.74%	27.94	96.24%	44.65	97.33%	39.27	97.70%	62.67	99.82%
8	2	45.36	90.32%	24.85	85.61%	41.38	90.21%	36.92	91.87%	62.68	99.84%
8	1	34.47	68.64%	15.41	53.08%	31.00	67.58%	27.68	68.88%	61.68	98.24%
6	8	49.32	98.21%	27.92	96.17%	44.72	97.48%	39.10	97.28%	62.90	100.18%
5	8	49.08	97.72%	27.75	95.60%	44.29	96.56%	38.76	96.45%	62.87	100.13%
4	8	46.40	92.39%	25.20	86.82%	41.81	91.14%	36.71	91.34%	62.74	99.93%
2	8	45.08	89.77%	23.67	81.55%	40.44	85.31%	35.31	87.85%	62.82	100.06%
1	8	39.81	79.26%	18.23	62.79%	35.39	77.14%	29.97	74.56%	62.83	100.07%
6	6	48.47	96.51%	26.82	92.38%	43.88	95.66%	38.38	95.49%	62.81	100.04%
5	5	47.55	94.68%	26.62	91.72%	43.13	94.02%	37.99	94.51%	62.67	99.81%
4	4	42.33	84.28%	23.12	79.64%	39.89	86.95%	33.39	83.08%	62.71	99.88%
2	2	39.69	79.02%	19.14	65.92%	35.49	77.36%	30.90	76.89%	62.79	100.00%
1	1	22.98	45.75%	6.09	20.99%	20.52	44.74%	18.36	45.69%	61.90	98.58%

Table 20: The relation between pruning asymmetry and symmetry for a FLAN-T5 base model on the Query Independent Web Snippets Abstractive Summarization Dataset

l_{enc}	l_{dec}	R-1	Impact	R-2	Impact	RSL	Impact	R-L	Impact	GenL	Impact
12	12	54.84	0.00%	34.19	0.00%	50.38	0.00%	44.68	0.00%	62.91	0.00%
12	10	55.02	0.33%	34.00	-0.56%	50.20	-0.35%	44.67	-0.02%	62.79	-0.19%
12	8	55.97	2.05%	34.50	0.91%	51.12	1.48%	44.90	0.48%	62.75	-0.24%
12	6	54.54	-0.55%	33.70	-1.42%	49.94	-0.87%	44.19	-1.11%	62.81	-0.16%
12	4	52.64	-4.01%	31.93	-6.62%	47.28	-6.16%	42.98	-3.81%	62.85	-0.09%
12	2	49.02	-10.61%	28.05	-17.97%	44.98	-10.71%	40.36	-9.68%	62.89	-0.02%
10	12	54.23	-1.11%	33.57	-1.82%	49.93	-0.89%	44.00	-1.52%	62.87	-0.05%
8	12	54.02	-1.50%	33.06	-3.31%	49.49	-1.76%	43.80	-1.96%	62.85	-0.09%
6	12	48.74	-11.13%	32.23	-5.72%	48.74	-3.26%	42.92	-3.95%	62.82	-0.14%
4	12	47.93	-12.61%	27.47	-19.65%	46.21	-8.28%	39.77	-11.00%	62.79	-0.19%
2	12	47.45	-13.48%	25.57	-25.22%	43.20	-14.26%	37.69	-15.66%	62.77	-0.22%
10	10	54.25	-1.08%	32.88	-3.82%	49.51	-1.72%	43.24	-3.23%	62.82	-0.13%
8	8	53.89	-1.73%	32.81	-4.04%	49.32	-2.10%	43.77	-2.04%	62.82	-0.14%
6	6	50.26	-8.34%	28.70	-16.05%	45.62	-9.45%	40.05	-10.37%	62.82	-0.13%
4	4	47.77	-12.89%	26.53	-22.40%	43.34	-13.97%	37.85	-15.29%	62.84	-0.10%
2	2	39.59	-27.80%	19.64	-42.57%	35.80	-28.95%	31.38	-29.78%	62.85	-0.09%

Table 21: The relation between pruning asymmetry and symmetry for a FLAN-T5 large model on the Query Independent Web Snippets Abstractive Summarization Dataset

l_{enc}	l_{dec}	R-1	Impact	R-2	Impact	RSL	Impact	R-L	Impact	GenL	Impact
24	24	57.81	100.00%	37.37	100.00%	53.14	100.00%	48.16	100.00%	62.85	100.00%
24	20	58.21	100.69%	37.59	100.59%	53.44	100.58%	48.46	100.62%	62.80	99.91%
24	16	57.25	99.04%	36.56	97.84%	52.71	99.19%	47.71	99.06%	62.83	99.97%
24	12	56.78	98.21%	35.74	95.64%	52.34	98.49%	46.81	97.18%	62.78	99.88%
24	8	56.19	97.19%	35.13	94.01%	51.59	97.08%	45.68	94.85%	62.79	99.90%
24	4	54.53	94.32%	33.69	90.15%	50.00	94.10%	44.65	92.71%	62.83	99.97%
20	24	57.34	99.19%	36.39	97.38%	52.66	99.10%	47.28	98.18%	62.81	99.93%
16	24	56.26	97.33%	35.90	96.07%	51.04	96.04%	46.82	97.22%	62.81	99.93%
12	24	55.31	95.67%	34.22	91.58%	50.60	95.23%	45.11	93.66%	62.88	100.04%
8	24	54.80	94.79%	33.42	89.43%	49.95	94.00%	44.11	91.59%	62.70	99.76%
4	24	51.40	88.92%	30.31	81.11%	46.49	87.48%	41.12	85.38%	62.70	99.75%
20	20	56.81	98.28%	36.32	97.20%	52.21	98.25%	46.82	97.21%	62.69	99.74%
16	16	56.10	97.05%	35.98	96.29%	51.05	96.07%	45.89	95.28%	62.71	99.76%
12	12	54.16	93.70%	33.00	88.31%	49.58	93.31%	44.80	93.02%	62.77	99.87%
8	8	51.77	89.55%	30.78	82.38%	47.31	89.03%	41.32	85.79%	62.73	99.81%
4	4	45.70	79.06%	22.77	60.94%	41.36	77.84%	36.09	74.94%	62.70	99.76%

Table 22: The relation between pruning asymmetry and symmetry for a FLAN-T5 small model on the Extreme Summarization (XSUM) Abstractive Summarization Dataset

l_{enc}	l_{dec}	R-1	Impact	R-2	Impact	RSL	Impact	R-L	Impact	GenL	Impact
8	8	33.27	0.00%	11.09	0.00%	26.17	0.00%	26.17	0.00%	28.01	0.00%
8	6	33.79	1.56%	11.61	4.74%	26.73	2.14%	26.74	2.18%	27.79	-0.78%
8	5	33.47	0.61%	11.43	3.12%	26.64	1.81%	26.65	1.83%	27.40	-2.18%
8	3	33.04	-0.69%	11.24	1.36%	26.26	0.36%	26.27	0.38%	28.08	0.26%
8	2	31.48	-5.36%	10.53	-5.02%	25.39	-2.99%	25.38	-3.01%	26.58	-5.13%
8	1	23.16	-30.39%	6.03	-45.58%	19.02	-27.32%	19.02	-27.33%	36.68	30.93%
5	8	33.31	0.13%	11.18	0.82%	26.16	-0.04%	26.16	-0.06%	28.31	1.08%
5	8	32.55	-2.15%	10.61	-4.32%	25.50	-2.55%	25.50	-2.55%	28.35	1.19%
3	8	31.82	-4.36%	10.11	-8.84%	24.92	-4.78%	24.92	-4.77%	28.43	1.50%
2	8	29.65	-10.87%	8.59	-22.48%	23.02	-12.02%	23.02	-12.03%	27.90	-0.39%
1	8	28.46	-14.46%	7.70	-30.57%	22.09	-15.60%	22.09	-15.59%	27.87	-0.50%
6	6	32.50	-2.29%	10.73	-3.24%	25.67	-1.90%	25.68	-1.88%	28.07	0.19%
5	5	31.77	-4.50%	10.19	-8.04%	25.14	-3.94%	25.14	-3.95%	28.09	0.29%
3	3	30.42	-8.57%	9.50	-14.31%	24.16	-7.66%	24.16	-7.67%	27.91	-0.38%
2	2	26.71	-19.70%	7.31	-34.09%	21.38	-18.30%	21.38	-18.31%	26.35	-5.93%
1	1	19.54	-41.26%	4.00	-63.91%	16.00	-38.86%	16.00	-38.87%	35.73	27.54%

Table 23: The relation between pruning asymmetry and symmetry for a FLAN-T5 base model on the Extreme Summarization (XSUM) Abstractive Summarization Dataset

l_{enc}	l_{dec}	R-1	Impact	R-2	Impact	RSL	Impact	R-L	Impact	GenL	Impact
12	12	38.78	0.00%	15.69	0.00%	31.14	0.00%	31.15	0.00%	25.92	0.00%
12	10	38.46	-0.83%	15.27	-2.65%	30.70	-1.43%	30.71	-1.42%	26.72	3.11%
12	8	38.11	-1.72%	14.91	-4.97%	30.34	-2.59%	30.34	-2.60%	27.64	6.65%
12	6	38.55	-0.58%	15.40	-1.83%	30.87	-0.87%	30.88	-0.87%	27.42	5.80%
12	4	38.04	-1.91%	15.19	-3.18%	30.63	-1.64%	29.65	-4.82%	26.40	1.85%
12	2	35.39	-8.74%	13.73	-12.47%	28.96	-7.02%	28.96	-7.03%	27.55	6.32%
10	12	39.04	0.68%	15.92	1.47%	31.22	0.24%	31.23	0.25%	26.89	3.75%
8	12	37.05	-4.45%	14.10	-10.09%	29.29	-5.95%	29.30	-5.93%	27.68	6.82%
6	12	36.45	-6.01%	13.84	-11.79%	28.96	-7.02%	28.96	-7.02%	27.21	4.99%
4	12	34.32	-11.48%	12.10	-22.88%	26.99	-13.35%	26.99	-13.34%	27.20	4.94%
2	12	31.88	-17.78%	10.27	-34.53%	24.85	-20.21%	24.85	-20.22%	28.22	8.88%
10	10	38.80	0.05%	15.72	0.22%	31.07	-0.25%	31.08	-0.23%	26.92	3.88%
8	8	37.21	-4.04%	14.30	-8.85%	29.55	-5.13%	29.54	-5.15%	27.40	5.72%
6	6	34.92	-9.95%	12.44	-20.68%	27.56	-11.51%	27.57	-11.50%	27.72	6.96%
4	4	32.48	-16.24%	10.67	-31.95%	25.49	-18.15%	25.50	-18.14%	27.98	7.98%
2	2	27.44	-29.23%	7.74	-50.65%	21.95	-29.51%	21.96	-29.52%	29.38	13.38%

Table 24: The relation between pruning asymmetry and symmetry for a FLAN-T5 large model on the Extreme Summarization (XSUM) Abstractive Summarization Dataset

l_{enc}	l_{dec}	R-1	Impact	R-2	Impact	RSL	Impact	R-L	Impact	GenL	Impact
24	24	39.71	0.00%	16.34	0.00%	31.72	0.00%	31.72	0.01%	26.74	0.00%
24	20	43.18	8.74%	19.80	21.17%	35.21	11.01%	35.22	11.04%	25.91	-3.10%
24	16	42.73	7.59%	19.30	18.10%	34.76	9.58%	34.76	9.59%	26.40	-1.29%
24	12	42.34	6.61%	18.92	15.78%	34.52	8.84%	34.53	8.87%	25.49	-4.68%
24	8	41.30	4.00%	17.96	9.94%	33.73	6.34%	33.75	6.39%	25.02	-6.45%
24	4	39.55	-0.40%	16.47	0.77%	32.25	1.66%	32.25	1.68%	26.30	-1.64%
20	24	42.77	7.71%	19.43	18.90%	34.83	9.82%	34.84	9.83%	26.18	-2.09%
16	24	41.55	4.63%	18.33	12.17%	33.64	6.05%	33.65	6.07%	26.33	-1.53%
12	24	39.95	0.61%	16.90	3.40%	32.13	1.29%	32.14	1.31%	27.14	-100.00%
8	24	37.57	-5.39%	14.97	-8.38%	29.94	-5.61%	29.94	-5.60%	25.99	-100.00%
4	24	34.81	-12.35%	12.52	-23.36%	27.32	-13.86%	27.32	-13.86%	27.61	-100.00%
20	20	42.48	6.98%	19.18	17.39%	34.62	9.13%	34.62	9.13%	25.84	-3.36%
16	16	40.78	2.69%	17.56	7.44%	32.99	4.00%	33.00	4.02%	26.47	-1.00%
12	12	38.94	6.98%	15.89	-2.78%	31.21	-1.61%	31.22	-1.58%	26.59	-0.57%
8	8	34.65	-12.75%	12.15	-25.65%	27.36	-13.76%	27.36	-13.73%	28.16	5.30%
4	4	29.82	-24.91%	8.96	-45.14%	23.59	-25.62%	23.60	-25.60%	28.10	5.09%

Table 25: Role of model symmetry in inference efficiency on FLAN-T5 small model on the QIWS dataset

l_{enc}	l_{dec}	R-2	Impact	BS 1	STD	Speedup	BS 8	STD	Speedup	BS 16	STD	Speedup
8	8	29.03	0.00%	524	3.95	1.00	653	2.49	1.00	729	5.12	1.00
8	6	28.90	-0.45%	406	1.28	1.29	514	5.02	1.27	583	2.47	1.25
8	5	28.56	-1.60%	348	2.34	1.51	455	1.6	1.44	527	1.85	1.38
8	4	27.94	-3.76%	293	3.35	1.79	394	6.32	1.66	469	2.65	1.55
8	2	24.85	-14.39%	195	1.61	2.69	353	3.38	1.85	426	6.38	1.71
8	1	15.41	-46.92%	132	0.959	3.97	211	2.82	3.09	389	2.94	1.87
6	8	27.92	-3.83%	512	5.15	1.02	626	4.19	1.04	684	2.81	1.07
5	8	27.75	-4.40%	508	3.56	1.03	617	4.91	1.06	666	4.16	1.09
4	8	25.20	-13.18%	514	3.55	1.02	603	4.52	1.08	639	2.08	1.14
2	8	23.67	-18.45%	514	5.14	1.02	585	5.36	1.12	608	4.45	1.20
1	8	18.23	-37.21%	510	5.81	1.03	574	4.21	1.14	595	7.06	1.23
6	6	26.82	-7.62%	407	5.26	1.29	496	8.77	1.32	548	1.97	1.33
5	5	26.62	-8.28%	346	6.84	1.51	430	3.54	1.52	480	12.4	1.52
4	4	23.12	-20.36%	375	4.25	1.40	441	6.92	1.48	478	10.6	1.53
2	2	19.14	-34.08%	402	2.05	1.30	452	9.84	1.44	476	8.29	1.53
1	1	6.09	-79.01%	134	6.2	3.91	527	3.03	1.24	549	13.4	1.33

Table 26: Role of model symmetry in inference efficiency on FLAN-T5 base model on the QIWS dataset

l_{enc}	l_{dec}	R-2	Impact	BS 1	STD	Speedup	BS 8	STD	Speedup	BS 16	STD	Speedup
12	12	34.19	0.00%	746	11	1.00	1060	2.84	1.00	1310	6.8	1.00
12	10	34.00	-0.56%	625	3.27	1.19	943	4.69	1.12	1200	4.8	1.09
12	8	34.50	0.91%	523	2.19	1.43	814	4.23	1.30	1070	5.34	1.22
12	6	33.70	-1.42%	425	1.92	1.76	652	3.39	1.63	970	4.79	1.35
12	4	31.93	-6.62%	350	1.32	2.13	510	3.1	2.08	815	2	1.61
12	2	28.05	-17.97%	202	1.41	3.69	451	2.92	2.35	762	0.911	1.72
10	12	33.57	-1.82%	710	6.2	1.05	995	2.74	1.07	1290	4.2	1.02
8	12	33.06	-3.31%	690	5.72	1.08	953	5.72	1.11	1270	4.3	1.03
6	12	32.23	-5.72%	716	8	1.04	944	7.22	1.12	1080	5.29	1.21
4	12	27.47	-19.65%	710	1.75	1.05	911	10.1	1.16	1,000	8.84	1.31
2	12	25.57	-25.22%	706	5.4	1.06	862	7.11	1.23	921	7.04	1.42
10	10	32.88	-3.82%	633	11.6	1.18	915	11	1.16	1120	5.51	1.17
8	8	32.81	-4.04%	512	4.98	1.46	737	9.78	1.44	911	4.98	1.44
6	6	28.70	-16.05%	401	3.16	1.86	572	4.73	1.85	702	1.57	1.87
4	4	26.53	-22.40%	301	2.92	2.48	415	3.01	2.55	509	0.997	2.57
2	2	19.64	-42.57%	189	1.98	3.95	312	2.88	3.40	389	0.892	3.37

Table 27: Role of model symmetry in inference efficiency on FLAN-T5 large model on the QIWS dataset

l_{enc}	l_{dec}	R-2	Impact	BS 1	STD	Speedup	BS 8	STD	Speedup	BS 16	STD	Speedup
24	24	37.37	0.00%	1430	6.08	1.00	2240	4.81	1.00	3320	1.02	1.00
24	20	37.59	0.59%	1210	4.73	1.18	1990	6.89	1.13	3010	2.63	1.10
24	16	36.56	-2.16%	1000	2.70	1.43	1750	5.92	1.28	2710	1.57	1.23
24	12	35.74	-4.36%	795	6.61	1.80	1510	10.40	1.48	2400	1.59	1.38
24	8	35.13	-5.99%	585	4.99	2.44	1260	7.14	1.78	2090	7.17	1.59
24	4	33.69	-9.85%	373	1.16	3.83	1030	10.50	2.17	1790	1.72	1.85
20	24	36.39	-2.62%	1410	3.66	1.01	2130	10.90	1.05	3090	5.98	1.07
16	24	35.90	-3.93%	1395	3.52	1.03	2060	9.89	1.09	2880	3.32	1.15
12	24	34.22	-8.42%	1380	5.20	1.04	1900	9.65	1.18	2630	0.81	1.26
8	24	33.42	-10.57%	1370	5.49	1.04	1790	19.00	1.25	2400	1.34	1.38
4	24	30.31	-18.89%	1350	7.33	1.06	1670	5.30	1.34	2170	2.79	1.53
20	20	36.32	-2.80%	1200	5.37	1.19	1880	7.89	1.19	2780	1.15	1.19
16	16	35.98	-3.71%	1020	3.49	1.40	1530	5.62	1.46	2230	1.80	1.49
12	12	33.00	-11.69%	749	5.30	1.91	1160	2.94	1.93	1710	0.89	1.94
8	8	30.78	-17.62%	650	3.32	2.20	970	2.78	2.31	1550	0.79	2.14
4	4	22.77	-39.06%	585	2.23	2.44	890	3.21	2.52	1450	0.92	2.29

Table 28: Role of model symmetry in inference efficiency on FLAN-T5 small model on the CNNDM dataset

l_{enc}	l_{dec}	R-2	Impact	BS 1	STD	Speedup	BS 8	STD	Speedup	BS 16	STD	Speedup
8	8	17.55	0.00%	138	5.05	1.00	230	7.61	1.00	330	3.71	1.00
8	6	17.68	0.74%	133	0.292	1.04	211	0.425	1.09	300	0.954	1.10
8	5	17.27	-1.64%	116	0.196	1.19	193	0.448	1.19	279	0.537	1.18
8	4	16.40	-6.57%	98.1	0.242	1.41	174	0.153	1.32	259	0.424	1.27
8	2	15.35	-12.58%	63.2	0.207	2.18	137	0.1	1.68	218	0.303	1.51
8	1	11.33	-35.43%	45.7	0.106	3.02	118	0.0827	1.95	198	0.148	1.67
6	8	17.69	0.81%	166	0.303	0.83	230	1.42	1.00	303	1.06	1.09
5	8	17.35	-1.16%	165	0.267	0.84	219	0.521	1.05	283	1.13	1.17
4	8	16.80	-4.30%	164	0.185	0.84	211	0.89	1.09	265	1.85	1.25
2	8	15.54	-11.49%	162	332	0.85	191	0.332	1.20	226	625	1.46
1	8	13.31	-24.17%	161	0.626	0.86	180	0.423	1.28	206	0.55	1.60
6	6	17.07	-2.77%	131	0.617	1.05	192	0.247	1.20	261	0.768	1.26
5	5	16.20	-7.72%	113	0.306	1.22	164	0.642	1.40	220	1.36	1.50
4	4	14.91	-15.05%	95.1	0.0955	1.45	135	0.21	1.70	182	0.268	1.81
2	2	11.97	-31.83%	57.8	0.27	2.39	78.9	0.078	2.92	103	0.238	3.20
1	1	6.05	-65.55%	39.1	0.136	3.53	50.2	0.132	4.58	63.4	0.0845	5.21

Table 29: Role of model symmetry in inference efficiency on FLAN-T5 base model on the CNNDM dataset

l_{enc}	l_{dec}	R-2	Impact	BS 1	STD	Speedup	BS 8	STD	Speedup	BS 16	STD	Speedup
12	12	19.77	0.00%	199	3.74	1.00	550	3.81	1.00	931	2.09	1.00
12	10	19.92	0.76%	179	3.31	1.11	524	16.2	1.05	889	4.41	1.05
12	8	19.85	0.42%	155	4.50	1.28	493	14	1.12	884	3.61	1.05
12	6	18.85	-4.63%	126	1.95	1.58	449	5.88	1.22	800	4.59	1.16
12	4	18.68	-5.49%	99.2	1.02	2.01	405	1.41	1.36	737	5.06	1.26
12	2	16.48	-16.62%	75.3	0.85	2.64	372	1.98	1.48	697	4.55	1.34
10	12	19.92	0.76%	198	4.75	1.01	495	14.5	1.11	811	1.18	1.15
8	12	19.67	-0.50%	196	3.72	1.02	441	7.82	1.25	715	4.39	1.30
6	12	18.85	-4.63%	187	4.81	1.06	396	13.3	1.39	613	9.45	1.52
4	12	18.22	-7.86%	183	3.54	1.09	330	5.04	1.67	509	2.1	1.83
2	12	17.06	-13.73%	176	3.52	1.13	272	1.79	2.02	400	3.25	2.33
10	10	19.72	-0.26%	171	3.21	1.16	462	11.9	1.19	776	4.62	1.20
8	8	19.17	-3.01%	141	2.97	1.41	37	12.1	14.86	628	6.48	1.48
6	6	17.46	-11.71%	109	1.71	1.83	281	2.61	1.96	478	3.55	1.95
4	4	15.87	-19.74%	82.5	1.24	2.41	198	1.71	2.78	329	0.74	2.83
2	2	12.23	-38.12%	50.7	1.30	3.93	112	2.59	4.91	178	0.557	5.23

Table 30: Role of model symmetry in inference efficiency on FLAN-T5 LARGE model on the CNNDM dataset

l_{enc}	l_{dec}	R-2	Impact	BS 1	STD	Speedup	BS 8	STD	Speedup	BS 16	STD	Speedup
24	24	21.15	0.00%	445	2.35	1.00	1480	20.1	1.00	2700	7.22	1.00
24	20	21.30	0.69%	390	33.7	1.14	1390	4.24	1.06	2590	7.7	1.04
24	16	21.32	0.81%	335	13.9	1.33	1330	7.7	1.11	2470	7.42	1.09
24	12	21.08	-0.34%	270	3.28	1.65	1250	11	1.18	2340	6.68	1.15
24	8	20.67	-2.27%	219	8.67	2.03	1180	8.17	1.25	2220	4.25	1.22
24	4	19.49	-7.88%	165	1.81	2.70	1090	6.6	1.36	2090	9.15	1.29
20	24	21.13	-0.12%	418	13.8	1.06	1320	15.3	1.12	2400	7.26	1.13
16	24	20.83	-1.53%	421	16.8	1.06	1150	16	1.29	2080	6.07	1.30
12	24	20.53	-2.94%	391	12.5	1.14	1000	21.7	1.48	1750	8.18	1.54
8	24	19.74	-6.67%	373	13.1	1.19	882	6.92	1.68	1430	4.79	1.89
4	24	18.68	-11.69%	350	4.32	1.27	670	15	2.21	1110	3.21	2.43
20	20	21.23	0.34%	359	4.3	1.24	1240	15.3	1.19	2260	6.73	1.19
16	16	20.90	-1.19%	1289	2.5	0.35	994	21.6	1.49	1820	4.27	1.48
12	12	20.13	-4.84%	229	12.1	1.94	756	12.6	1.96	1370	4.6	1.97
8	8	18.47	-12.70%	160	31.8	2.78	513	2.55	2.88	926	7.24	2.92
4	4	15.51	-26.68%	89.7	0.588	4.96	267	2.14	5.54	479	4.3	5.64

Table 31: Role of model symmetry in inference efficiency on FLAN-T5 small model on the XSUM dataset

l_{enc}	l_{dec}	R-2	Impact	BS 1	STD	Speedup	BS 8	STD	Speedup	BS 16	STD	Speedup
8	8	11.09	0.00%	135	2.73	1.00	227	3.51	1.00	332	1.91	1.00
8	6	11.61	4.74%	108	1.70	1.25	196	1.94	1.16	303	7.95	1.10
8	5	11.43	3.12%	94.1	3.02	1.43	183	3.43	1.24	281	6.77	1.18
8	4	11.24	1.36%	82.7	2.66	1.63	168	2.33	1.35	263	2.24	1.26
8	2	10.53	-5.02%	55.8	1.72	2.42	141	1.53	1.61	234	5.01	1.42
8	1	6.03	-45.58%	41.1	0.64	3.28	124	0.414	1.83	215	4.69	1.54
6	8	11.18	0.82%	133	3.51	1.02	204	3.63	1.11	295	5.72	1.13
5	8	10.61	-4.32%	134	3.42	1.01	193	3.76	1.18	273	10.4	1.22
4	8	10.11	-8.84%	130	2.77	1.04	185	13.6	1.23	245	6.45	1.36
2	8	8.59	-22.48%	126	4.77	1.07	163	6	1.39	203	4.1	1.64
1	8	7.70	-30.57%	126	3.38	1.07	148	2.02	1.53	180	2.85	1.84
6	6	10.73	-3.24%	104	0.45	1.30	178	3.24	1.28	254	2.37	1.31
5	5	10.19	-8.04%	91.6	2.10	1.47	151	1.78	1.50	219	10.3	1.52
4	4	9.50	-14.31%	79	3.38	1.71	124	2.42	1.83	178	1.59	1.87
2	2	7.31	-34.09%	49.5	2.56	2.73	74.8	1.9	3.03	101	0.719	3.29
1	1	4.00	-63.91%	32	1.25	4.22	48.7	2.11	4.66	61.9	1.81	5.36

Table 32: Role of model symmetry in inference efficiency on FLAN-T5 base model on the XSUM dataset

l_{enc}	l_{dec}	R-2	Impact	BS 1	STD	Speedup	BS 8	STD	Speedup	BS 16	STD	Speedup
12	12	15.69	0.00%	205	3.81	1.00	546	8.7	1.00	917	4.72	1.00
12	10	15.27	-2.65%	171	2.79	1.20	508	6.39	1.07	876	3.02	1.05
12	8	14.91	-4.97%	150	1.32	1.37	476	2.82	1.15	830	1.08	1.10
12	6	15.40	-1.83%	129	4.33	1.59	450	9.33	1.21	789	3.73	1.16
12	4	15.19	-3.18%	101	2.16	2.03	411	5.27	1.33	744	1.71	1.23
12	2	13.73	-12.47%	76	1.76	2.70	380	3.43	1.44	706	8.13	1.30
10	12	15.92	1.47%	200	6.37	1.03	494	2.45	1.11	818	1.72	1.12
8	12	14.10	-10.09%	195	5.47	1.05	445	20.8	1.23	713	1.71	1.29
6	12	13.84	-11.79%	190	3.89	1.08	396	9.79	1.38	612	4.64	1.50
4	12	12.10	-22.88%	185	2.24	1.11	337	3.09	1.62	505	1.96	1.82
2	12	10.27	-34.53%	180	2.08	1.14	282	4.03	1.94	399	2.85	2.30
10	10	15.72	0.22%	174	4.09	1.18	475	18.5	1.15	772	1.79	1.19
8	8	14.30	-8.85%	140	1.95	1.46	373	2.21	1.46	625	1.51	1.47
6	6	12.44	-20.68%	112	1.71	1.83	290	6.77	1.88	480	3.5	1.91
4	4	10.67	-31.95%	84.2	3.75	2.43	201	1.58	2.72	330	4.43	2.78
2	2	7.74	-50.65%	51.5	3.01	3.98	112	1.02	4.88	179	0.894	5.12

Table 33: Role of model symmetry in inference efficiency on FLAN-T5 large model on the XSUM dataset

l_{enc}	l_{dec}	R-2	Impact	BS 1	STD	Speedup	BS 8	STD	Speedup	BS 16	STD	Speedup
24	24	16.34	0.00%	447	19.4	1.00	1480	23	1.00	2700	16.1	1.00
24	20	19.80	21.16%	374	4.84	1.20	1410	17.5	1.05	2580	7.52	1.05
24	16	19.30	18.09%	327	19.4	1.37	1320	8.18	1.12	2460	7.19	1.10
24	12	18.92	15.77%	272	7.91	1.64	1240	7.06	1.19	2340	7.5	1.15
24	8	17.96	9.93%	216	7.81	2.07	1170	11.4	1.26	2210	6.49	1.22
24	4	16.47	0.76%	165	3.11	2.71	1090	3.66	1.36	2080	7.17	1.30
20	24	19.43	18.88%	406	21.5	1.10	1310	11.5	1.13	2390	7.76	1.13
16	24	18.33	12.16%	412	20.3	1.08	1140	6.88	1.30	2080	7.01	1.30
12	24	16.90	3.39%	384	18.8	1.16	986	11	1.50	1750	686	1.54
8	24	14.97	-8.39%	369	8.87	1.21	822	15.5	1.80	1420	15.5	1.90
4	24	12.52	-23.37%	345	4.41	1.30	649	3.26	2.28	110	5.96	24.55
20	20	19.18	17.38%	357	11.8	1.25	1230	13.2	1.20	2260	2.16	1.19
16	16	17.56	7.43%	288	5.91	1.55	995	9.41	1.49	1820	5.33	1.48
12	12	15.89	-2.79%	217	3.09	2.06	748	3.25	1.98	1370	6.59	1.97
8	8	12.15	-25.66%	158	6.04	2.83	511	9.62	2.90	920	2.06	2.93
4	4	8.96	-45.14%	92.3	2.88	4.84	267	1.51	5.54	481	1.69	5.61